Journal of Molecular Catalysis A: Chemical 383–384 (2014) 159–166

Contents lists available at ScienceDirect

Journal of Molecular Catalysis A: Chemical

journal homepage: www.elsevier.com/locate/molcata

Synthesis and application of Fe^{III}, Ni^{II} and Mn^{II} complexes anchored to HMS as efficient catalysts for cycloalkane oxyfunctionalization

Kelly Machado, Pedro B. Tavares, Gopal S. Mishra*

Laboratory of Materials, Centro de Química-Vila Real (CQ-VR), Department of Chemistry, University of Trás-os-Montes and Alto Douro (UTAD), Vila Real 5001-801, Portugal

ARTICLE INFO

Article history:
Received 8 April 2013
Received in revised form 31 October 2013
Accepted 1 December 2013
Available online 15 December 2013

Keywords:
Supported catalyst
Cyclohexane
O_2 oxidation
Batch reactor
Radical mechanism

ABSTRACT

Methoxysilane Schiff-base pentacoordinate metal complexes, *i.e.* Fe[Sal(PMeO-Si)DPTA], Ni[Sal(PMeO-Si)DPTA] and Mn[Sal(PMeO-Si)DPTA], were synthesized and single site covalently anchored into the uniform porous texture of HMS (2–10 nm size) *via* condensation process. The correspondent supported catalysts (**4.a**, **4.b** and **4.c**, respectively) were characterized by FT-IR, SEM/EDS, XRD, TG, EPR and AAS analysis. In the catalytic tests, they showed high efficiency in the selective oxidation of cyclohexane using molecular O_2 (overall conversion 40.7% with Cat. **4.a**, 29.5% with Cat. **4.b** and 26.2% with Cat. **4.c**) under relatively mild condition in batch reactor. The Cat. **4.a** system (HMS/**3.a**) exhibits highest TONs *ca.* 4.2×10^3 with good selectivity *ca.* 70% (48% ketone selectivity). The reaction mechanism involves free radicals, as it was proved by the addition of PPh_3. Finally, these supported catalysts could be reuse up to several catalytic cycles.

1. Introduction

The activation C—H bond of hydrocarbons with molecular oxygen is an important reaction since several industrial processes are based on this transformation [1–4]. The use of molecular O_2 in the catalysis of alkanes oxidation is much attractive due to its low price, readily availability in atmospheric air as "greener oxidant" [5] and less toxic compared to other oxygen donors: H_2O_2, *t*-BuOOH, *etc.* [6,7]. In particular, Schiff bases ligands are able to stabilize many different metals in various oxidation states [8–11], controlling the performance of metals in a large range of valuable catalytic transformations [12,13]. Nevertheless, homogeneous catalysts must be separated later from the reaction mixture, which is a cost of the process and difficult to recycle. To improve the method, one must immobilize the metal complexes catalysts on solid supports, preventing the requirement for laborious and inefficient extraction processes. The activity of this type of catalyst is mainly dependent upon the structure of complex, surface area of support and substrate polarity which are the requirements for the reactants to be in contact on the active catalyst centre [14]. In the case of using high surface area mesoporous support, the inorganic complexes have been anchored through the interaction between the silanol of the supporting matrix and terminal reactive groups of the complex, yielding supported hybrid catalysts [15–17]. Some such supported catalysts might be considered, namely due to their easy separation from the product (by simple filtration), the possibility of recycling them and the facility to control and tune the catalyst composition.

For the current process, we have chosen cyclohexane because it oxidizes to alcohol and ketone products, also known as KA oil. These product are further convert to adipic acid and caprolactam, which are the key components for the production of urethane foams, polyamide-6, lubricating additives and nylon-6 [18]. Typically, Co slats have been used in the industrial cyclohexane oxidation either by air O_2 or pure O_2. At temperatures above 423 K low conversions (*ca.* 4%) but 85% selectivity (KA oil) was achieved [19]. This way, industrial cyclohexane oxidation uses inherently inefficient methodology that necessitates repeated recycling of feedstock. The alternative use of peroxides is expensive and is also accompanied by the formation of toxic by-products [20–22]. The establishment of a greener and more effective cyclohexane oxidation process by the using of atmospheric oxygen is therefore a present need.

In past few years, metal cations or often oxides have been incorporated on inorganic materials (*e.g.* zeolites, silica, alumina or aluminophosphates), while promoters have been used to reduce the induction period and to increase the selectivity for the targeted product of cyclohexane [23–25]. Metal-substituted heteropoly compounds (heteropolyoxometalates) catalysts demonstrated good activity towards alkanes oxidation [26]. Re complexes over SiO_2 and Pd–Re over Al_2O_3 have also demonstrated considerably good catalytic activities for the oxidation of cycloalkane [27,28]. The SiO_2 supported di(ethylthio)alkane Pd complexes give 16.2% conversion and 98% selectivity [29]. The Y-type zeolite anchored V and

* Corresponding author. Fax: +351 259350286.
E-mail addresses: mishrags@utad.pt, mishrags@gmail.com (G.S. Mishra).

1381-1169/$ – see front matter © 2013 Elsevier B.V. All rights reserved.
http://dx.doi.org/10.1016/j.molcata.2013.12.004

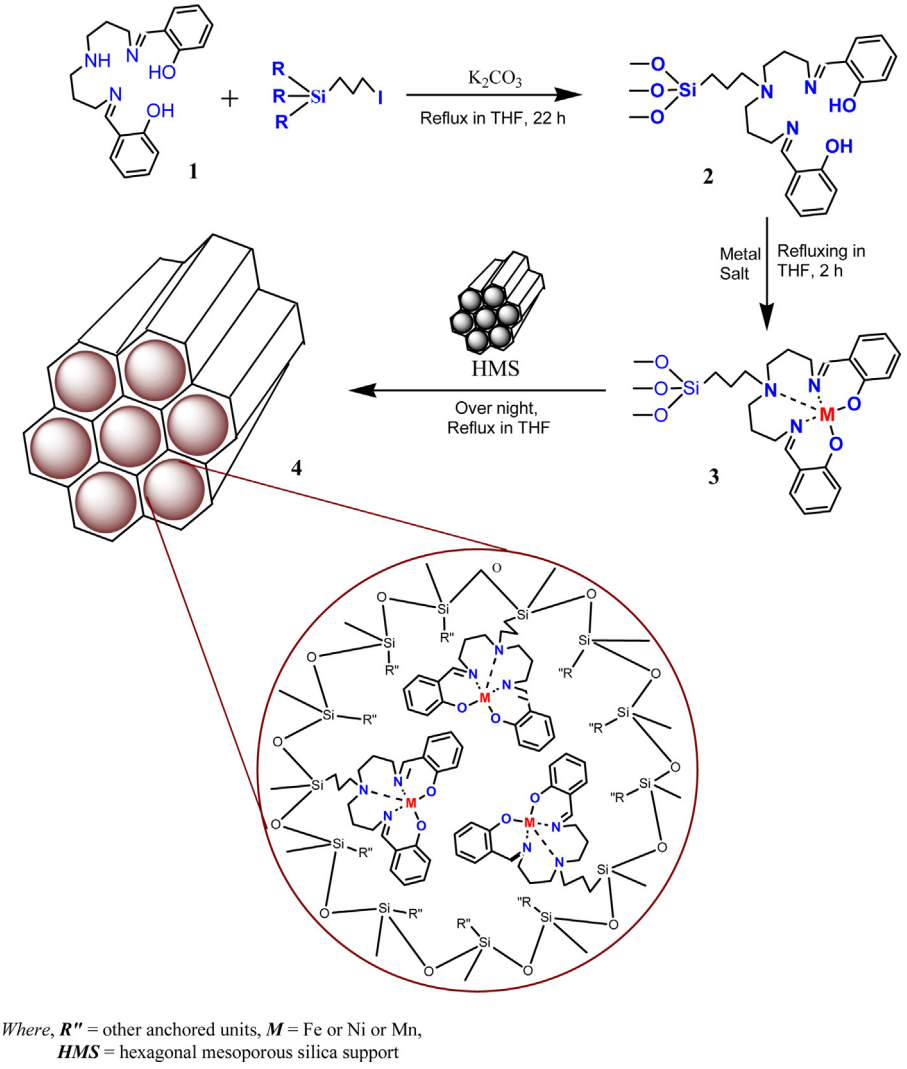

Scheme 1. Synthesis procedure of Schiff-base trimethoxysilane pentacoordinate metal complexes and single site anchoring into the uniform porous texture of HMS.

Cu salen complex catalysts were applied in the cyclohexane/H_2O_2 process and achieved 86.6% and 18.1% conversions with V and Cu catalysts, respectively [30]. The Fe and Mn complexes were also tested in the cyclohexane oxidation study and obtained 10.2% conversion with Fe complex and *t*-BuOOH [31]. Previously, we had also prepared same type of pentacoordinate Schiff base ligands of V-complexes over SiO_2 and tested in cyclohexane O_2 oxidation and obtained 36% conversion with 98% product selectivity [32]. Some other maltolato type of V-complexes supported SiO_2 were also applied and obtained relatively low conversion 15% [33]. Alumina supported hetero binuclear macrocyclic Co–V complex and SiO_2 anchored Schiff base Co complexes catalysts have been investigated obtaining 20% conversion in both the cases [34,35]. These results show that the use of non precious metals in catalysts is favourable due to low price, resistance to temperature and light. Its strongly motivate the investigation of low cost catalysts.

Hence, the main target of this study is to synthesize and to apply novel methoxysilane Schiff-base Fe^{III}, Ni^{II} and Mn^{II} complexes for the easy anchoring (without any linker) over hexagonal mesoporous silica (HMS) as heterogeneous catalyst. These catalysts are tested for the gas–liquid oxidation of cyclohexane with molecular O_2 under relatively mild condition to obtain high conversion with product selectivity.

2. Experimental

2.1. General materials and methods

A standard Schlenk technique was used for the synthesis of Fe, Ni and Mn complexes under normal atmospheric conditions. All the chemicals and solvents *i.e.* ethanol (EtOH), *n*-pentane, toluene, diethyl ether (Et_2O), acetonitrile (MeCN), tetrahydrofuran (THF) and cyclohexane (Cy-hx) were from Janssen Chemicals. 3-Idopropyl trimethoxysilane (PMeO-Si), salicylaldehyde (Sal), bis(2,4-pentanedionato)cobalt, bis(aminopropyl)amine (DPTA), potassium carbonate (K_2CO_3), iron chloride anhydrous ($FeCl_3$), nickel acetylacetonate ($C_{10}H_{14}NiO_4$), manganese acetate [$Mn(CH_3COO)_2$], *n*-hydroxyphthalimide (*n*-NIPH) and tetraethylorthosilicate (TOS) were from Sigma–Aldrich and they were used as received.

2.2. Catalyst preparation

Ligand **2** (Scheme 1), Sal(PMeO-Si)DPTA, was prepared as described earlier [32,36], starting from equimolar quantities of bis(salicylidenimino-3-propyl)amine and 3-idopropyl trimethoxysilane, in THF reflux, in the presence of K_2CO_3.

2.2.1. Synthesis of Fe[Sal(PMeO-Si)DPTA], ***3.a***

The complex **3.a** was synthesized by adding $FeCl_3.6H_2O$ (4.38×10^{-3} mmol) (in THF 30 mL solution) to a THF solution (20 mL) of ligand **2** (4.99×10^{-3} mmol), with constant stirring. The red mixture was heated and refluxed for 2 h. The final solution was concentrated and upon addition of *n*-pentane a red solid precipitated. The solid was filtered, washed with *n*-pentane and dried under vacuum to obtain **3.a** complex (88% yield, Scheme 1). It is soluble in polar organic solvents. Anal. calcd. for $FeC_{\mathbf{26}}H_{\mathbf{37}}N_{\mathbf{3}}O_{\mathbf{5}}Si$: C, 56.24; H, 6.66; N, 7.56. Found: C, 54.77; H, 6.12; N, 6.21. FT-IR (KBr pellet, cm^{-1}): ν = 3010 [s, ν (C—H)]; 29,505 [s, ν (C—H)]; 1620 and 1563 [s, (ν C=N) and s, (ν C=C)]; 1176 [s, (ν Si—OCH_3); 1064 [s, (ν C—N)] and 465 [ν (FeO)]. EPR (CH_2Cl_2, at 25 °C): g = 1.9982, $A^{\|}$ and $A^{\perp}$ (in $\times 10^{-4}$ cm^{-1}) = 1.62 and 59.8. FAB^+-MS: m/z = 555.19 [$(M+H)^+$, 100], 410 [$(M-(CH_{\mathbf{2}}Si(OCH_3)_{\mathbf{3}})^+$, 14], 1 [$(Si(OCH_3)_{\mathbf{3}})$, 99].

2.2.2. Synthesis of Ni[Sal(PMeO-Si)DPTA], ***3.b***

The complex **3.b** was synthesized by mixing a solution of $C_{10}H_{14}NiO_4$, m. wt. 256.91 (4.38×10^{-3} mmol) in THF (30 mL), to an equimolar amount of ligand **2** (4.99×10^{-3} mmol) in THF (20 mL). The green mixture was heated and refluxed for 2 h. The final solution was concentrated and upon addition of *n*-pentane a light green solid precipitated. The solid was collected by filtration, washed with *n*-pentane and dried under *vacuo* to obtain **3.b** complex (85% yield, Scheme 1). It is soluble in most of polar solvents but insoluble in Et_2O. Anal. calcd. for $NiC_{\mathbf{26}}H_{\mathbf{37}}N_{\mathbf{3}}O_{\mathbf{5}}Si$: C, 56.04; H, 6.64; N, 7.54. Found: C, 55.19; H, 6.32; N, 7.26. FT-IR (KBr pellet, cm^{-1}): ν = 3090 [s, ν (C—H)]; 2832 [s, ν (C—H)]; 1644 and 1564 [s, (ν C=N) and s, (ν C=C)]; 1136 [s, (ν Si—OCH_3) and 1066 [s, (ν C—N)]. EPR (CH_2Cl_2, at 25 °C): g = 1.9982, $A^{\|}$ and $A^{\perp}$ (in $\times 10^{-4}$ cm^{-1}) = 1.62 and 59.8. FAB^+-MS: m/z = 557.19 [$(M+H)^+$, 100], 415 [$(M-(CH_{\mathbf{2}}Si(OCH_3)_{\mathbf{3}})^+$, 14], 1.3 [$(Si(OCH_3)_{\mathbf{3}})$, 99].

2.2.3. Synthesis of Mn[Sal(PMeO-Si)DPTA], ***3.c***

The complex **3.c** was synthesized by mixing a solution of $Mn(OAc)_2$, m. wt. 173.01 (4.99×10^{-3} mmol) in THF (30 mL) to an equimolar amount of ligand **2** (4.99×10^{-3} mmol) in THF (20 mL). This reaction mixture was heated and refluxed for 2 h. The final solution was concentrated and upon addition of *n*-pentane a yellowish brown solid precipitated. The solid was collected by filtration, washed with *n*-pentane and dried under *vacuo* to obtain **3.c** complex (86% yield, Scheme 1). It is soluble in most of polar solvents but insoluble in Et_2O. Anal. calcd. for $MnC_{\mathbf{26}}H_{\mathbf{37}}N_{\mathbf{3}}O_{\mathbf{5}}Si$: C, 56.35; H, 6.68; N, 7.58. Found: C, 56.16; H, 6.31; N, 6.60. FT-IR (KBr pellet, cm^{-1}): ν = 3066 [s, ν (C—H)]; 2935 [s, ν (C—H)]; 1653 and 1574 [s, (ν C=N) and s, (ν C=C)]; 1142 [s, (ν Si—OCH_3) and 1072 [s, (ν C—N)]. EPR (CH_2Cl_2, at 25 °C): g = 1.9982, $A^{\|}$ and $A^{\perp}$ (in $\times 10^{-4}$ cm^{-1}) = 1.62 and 59.8. FAB^+-MS: m/z = 554.19 [$(M+H)^+$, 100], 416 [$(M-(CH_{\mathbf{2}}Si(OCH_3)_{\mathbf{3}})^+$, 14], 1.2 [$(Si(OCH_3)_{\mathbf{3}})$, 99].

2.2.4. Preparation of HMS support

The HMS was prepared according to earlier published method [37]. Tetraethoxysilane (TEOS, 37.0 cm^3, 0.166 mol) was added to a mixed solution of ethanol (88.1 cm^3, 1.51 mol), water (88.5 cm^3, 4.91 mol) and dodecylamine (10.3 cm^3, 0.0448 mol). During 24 h the mixture was stirred at room temperature and the white precipitate obtained was vacuum-filtered and washed with deionized water (100 cm^3) and ethanol (100 cm^3). The precipitate was dried and calcinated at 873 K for 24 h to remove the template and obtained uniform porous texture of HMS (*ca.* 2–10 nm size). The uniform porous texture structure was characterized by the XRD, SEM and with SEM–EDS.

2.2.5. Preparation of final catalyst

Each of the complexes **3.a**, **3.b** and **3.c** (50 mg) was dissolved in dry toluene (50 mL). Then HMS (1000 mg) was added and heated under reflux for 12 h in air. The obtained solids were washed in Soxhlet with toluene to remove any non-anchored complexes. The complex **3.a**, 45.6 mg, **3.b**, 46.0 mg and **3.c**, 44.8 mg were anchored into HMS. The final catalysts were recorded as Cat. **4.a** (HMS/**3.a**), Cat. **4.b** (HMS/**3.b**) and Cat. **4.c** (HMS/**3.c**). All the reaction manipulations were carried out under N_2 atmosphere due to sensitive alkyloxy group of the metal complexes.

2.2.6. Solid catalyst characterization

FT-IR (KBr pellet, cm^{-1}): broad shoulders were observed at *ca.* 3715–3345 cm^{-1} and 1330 to 930 cm^{-1} in all the supported catalysts (**4.a**–**4.c**) due to HMS effect. Some additional peaks of complexes on the support matrix were confirmed [s, (ν C=O at 2260–2200 cm^{-1}, NH bands at 1644–1540 cm^{-1} and Si—O bands 980–955 cm^{-1}. TGA: the supported Cat. **4.a** to **4.c** show slow weight losses above *ca.* 380 to 435 K, most likely due to the release of moisture. The second major weight loss of all the catalysts was observed above *ca.* 500 K due to partial decomposition of organic groups of metal complexes and complete weight loss of supported complex on HMS was obtained at about 670 K. AAS analysis: the metal content in the supported catalysts, Cat. **4.a**, **4.b** and **4.c**, were measured in the range of 0.20–0.35 weight %. BET: surface area result shows that HMS has 695 m^2/g surface area (pore volume 0.67 m^3/g). After the anchoring, it was reduced *i.e.* for Cat. **3.a** (474 m^2/g and pore volume 0.53 m^3/g), for Cat. **3.b** (756 m^2/g, pore volume 0.51 m^3/g) and for Cat. **3.c** (789 m^2/g, pore volume 0.57 m^3/g). EPR: for the catalysts samples **4.a**–**4.c** (at room temperature) EPR spectrum with range of g = 1.9998–1.9825 and range of $A^{\|}$ and $A^{\perp}$ (in $\times 10^{-4}$ cm^{-1}) = 153.2–164.7 and 59.6–61.8, were obtained, respectively. SEM/EDS analysis: morphological and chemical analysis of the Cat. **4.a**–**4.c** showed bright spotted metal rich areas.

2.2.7. Instrumentation

Infrared spectra (FT-IR, 4000–400 cm^{-1}) were recorded on a Unicam Research Series, spectrophotometer in KBr pellets). Elemental analyses (EA) were carried out on a Carlo Erba 1108 Analyzer by chromatographic combustion method. FAB mass spectra (FB-MS) were obtained on a Bruker Daltonics APEX-QE spectrophotometer in electron spray ESI mode (7 T superconducting magnet). The morphologies of the catalysts were analyzed by scanning electron microscopy (SEM) on FEI Quanta 400, equipped with an EDS detector (EDAX). X-ray diffraction patterns were collected in Bragg–Bentano and in low angle geometries. The measurements were performed on a Philips X'Pert MPD equipped with the ultrafast X'Celerator detector and secondary monochromator. A low angle accessory was used for 2θ measurements between 0.5 and 5°. A Micromeritices Gemini 2390 instrument was used for the determination of BET surface area and porosity of catalysts with N_2 gas physisorption to produce surface area and porosity results. A thermogravimetric analysis was performed in a TA Instruments Q50 thermogravimetric analyzer. EPR spectra were recorded in the X band Bruker ESP 300E spectrophotometer at room temperature and calibrated with diphenylpicrylhydrazyl (dpph). Atomic Absorption Spectroscopy (AAS) was used to determine the metal concentration on a Perkin-Elmer 41000ZL spectrophotometer (5 mg of sample was digested in HF + HNO_3). The reaction products were analyzed in gas chromatography (GC), FISONS GC-8000 series gas chromatograph equipped with a FID detector and a DB-WAX capillary column (length: 30 m; internal diameter: 0.32 mm). The reaction products were further identified by GC–MS using a Carlo-Erba Auto/HRGC/MS instrument.

2.3. Heterogeneous catalysis method and product analysis

A stainless steel rocking type batch reactor (38 cm^3 capacity), equipped with a gas inlet and a pressure gauge was used for the

oxidation reactions. The inner temperature of the reactor was monitored by a thermocouple. For each experiment, the reactor was charged with the substrate and catalyst, closed, the air was removed and O_2 introduced. After the reaction, the catalyst was separated from the liquid mixture by filtration, washed several times with acetonitrile and reactivated by air drying at 60 °C for 8 h, for further studies. The reaction products were quantitatively analyzed by GC (30 μL of pentanone added as internal standard to 1.0 mL of the filtered final reaction solution) and further identified by GC–MS.

Turn over numbers (TONs) was calculated as mole of product per mole of supported metal complex. The overall conversion was calculated as mol of product per mole of substrate and the selectivity calculated as mol of particular product per mole of the total products. Some additional experiments have been carried out for the detection of alkylperoxide radicals (ROOH) [32]. At the end of reaction, the final solution was treated with an excess of PPh_3 prior to GC analysis. The hydroperoxide still present is deoxygenated by PPh_3 to the alcohol ROH (with Ph_3PO formation), thus suppressing the ROOH decomposition to both Cy-ol and Cy-one in GC. Moreover, some oxidation reaction of cyclohexane has been treated with 4.0 mg of carbon ($CBrCl_3$) or oxygen- (Ph_2NH) radical traps to confirm the presence of alkyl or hydroperoxide radicals.

3. Results and discussion

3.1. Supported catalysts: synthesis and characterization

Our first approach was the synthesis of Schiff base trimethoxysilane pentacoordinate Fe^{III}, Ni^{II} and Mn^{II} complexes for the anchoring on mesoporous HMS support. These supported catalysts were applied for the cyclohexane oxidation process as recyclable catalysts. Hence, methoxysilane Schiff base ligand **2** was synthesized as according to F. Carré procedure [36], due to terminal alkyloxy reactive groups for direct anchoring into support. The Schiff base ligand have two donor sets of phenolate oxygen, two donor nitrogens and another tertiary amine nitrogen atom that have been reacted with the terminal iodine of the 3-iodopropyl-trimethoxysilane (obtained 87%, yield). The metal salts were separately introduced at the next step of synthesis process with ligand **2**, for the preparation of three types of complexes, *i.e.* Fe[Sal(PMeO-Si)DPTA], (yield 88%, **3.a**), Ni[Sal(PMeO-Si)DPTA] (yield 85%, **3.b**) and Mn[Sal(PMeO-Si)DPTA] (yield 86%, **3.c**). The proposed formulation for **3.a**–**3.c** complexes has been supported by elemental analysis, FT-IR, NMR, EPR and FAB-mass spectral data. The lone pair of electron was confirmed in the EPR spectra which shows the typical "*g*" value that was obtained in the range of 1.9998–1.9825 and $A^{\|}$ and $A^{\perp}$ (in $\times 10^{-4}$ cm^{-1}) in the range of 153.2–164.7 and 59.6–61.8. The Feb-Mass spectrum of each complex was characterized by an intense molecular ion, which is the most abundant ion in the spectrum, as well as relatively abundant doubly charged parent molecular ions. No polymeric species were detected in any spectrum which suggests that either the complexes are monomeric or any polymers present were destroyed upon sublimation or upon electron impact.

For the preparation of supported catalysts, a grafted reaction of the —OH of uniform porous texture HMS with the direct anchoring of $—OCH_3$ of complexes (**3.a**, **3.b** and **3.c)** in toluene medium by a condensation reaction was employed. Final supported hybrid catalysts were obtained as Cat. **4.a**, Cat. **4.b** and Cat. **4.c**. Since methoxysilane is moisture sensitive, all the manipulations have been carried out under N_2. Any residual and excess of complexes in toluene were subsequently removed in the Soxhlet. To the best of our knowledge, these supported catalysts are being described for the first time (Scheme 1).

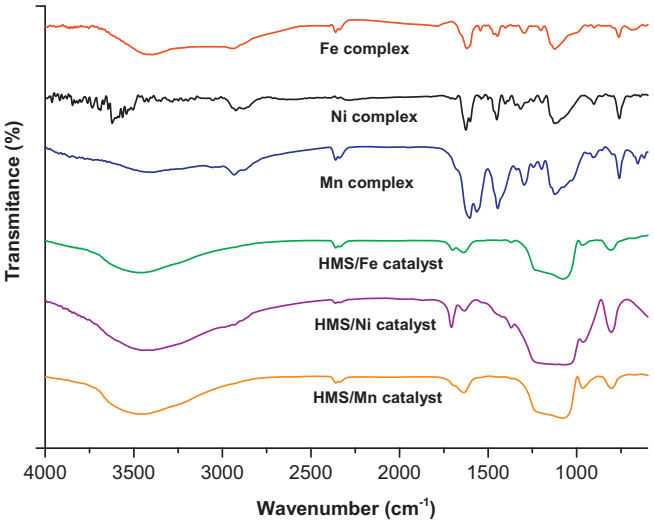

Fig. 1. FT-IR of metal complexes (**3.a**, **3.b** and **3.c**) and after anchoring of HMS as supported catalysts (Cat. **4.a**, **4.b** and **4.c**).

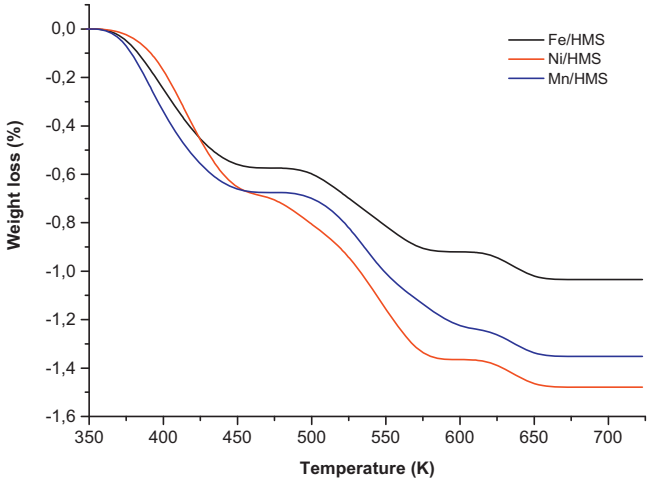

Fig. 2. TGA analysis results of single site anchored metal complex into HMS as supported catalysts (Cat. **4.a**, **4.b** and **4.c**).

All the anchored **3.a**, **3.b** and **3.c** complexes show a broad shoulder in FT-IR spectrum (Fig. 1), between; ν = 3715–3345 and ν = 1330–930 cm^{-1}, due to HMS effect. The presence of metal complexes over HMS matrix was confirmed by the additional bands *i.e.* C═O at 2260–2200 and C—N bands at 1644–1540 and Si—O bands at 980–955 cm^{-1}. The thermal stability of all the solid catalysts samples was analyzed by TGA (Fig. 2) showing 0.6% weight loss below 500 K due to moisture release, below the maximum reaction temperature (*i.e.* 473 K, Fig. 6). Additional weight loss (0.9%) from 500 K up to 700 K is due to complex decomposition. The BET surface result shows that initially HMS has 695 m^2/g surface area with the pore volume 0.67 m^3/g. After the anchoring of Cat. **3.a**, it was reduced 474 m^2/g and pore volume 0.53 m^3/g. The surface areas for other catalysts were obtained as 756 m^2/g, pore volume 0.51 m^3/g for Cat. **3.b** and 789 m^2/g, pore volume 0.57 m^3/g for Cat. **3.c**. Thus suggesting that the supported catalysts are stable in the range of the reaction temperatures studied. The metal content presence of Fe, Ni and Mn on the HMS were further confirmed in the AAS analysis and obtained 0.20–0.35 wt.% of fresh catalysts. After the catalytic reaction, the most active Cat. **4.a** shows a small amount 1.32 wt.% of metal leaching.

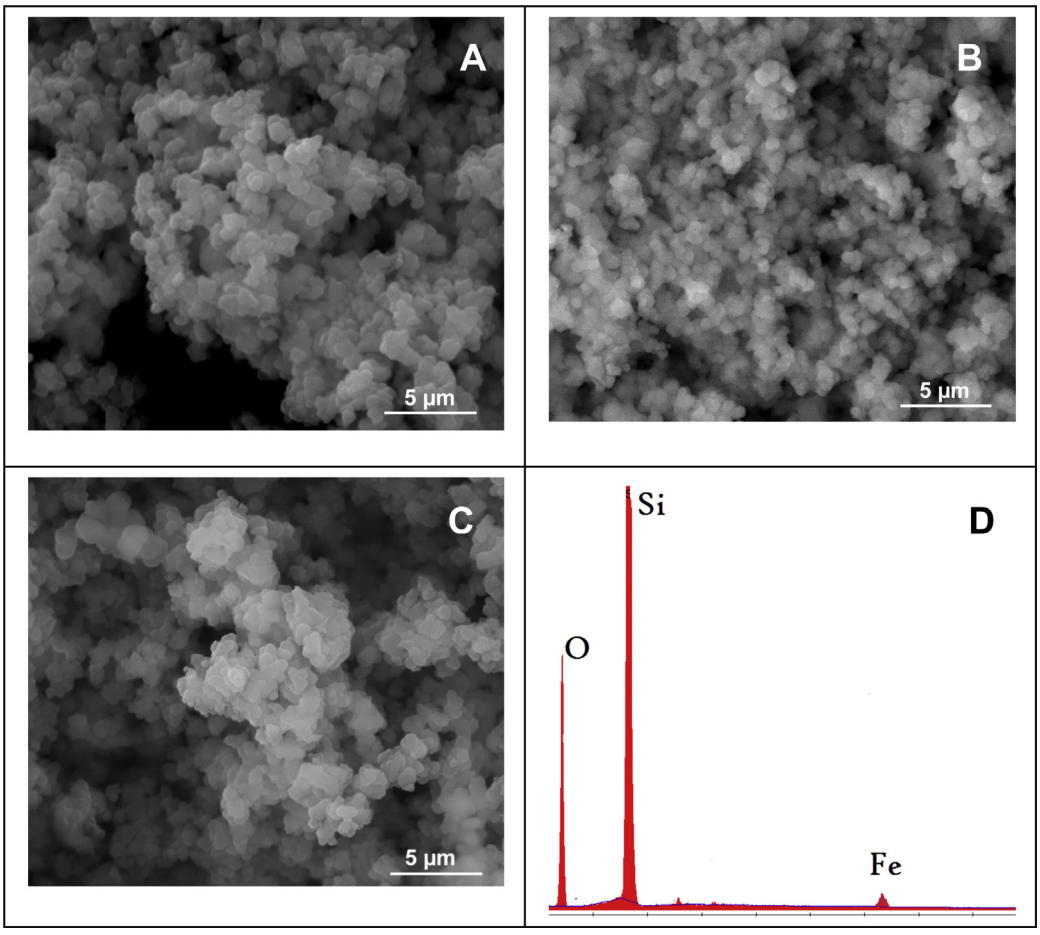

Fig. 3. SEM image of HMS Fig. A of Cat. **4.a**, Fig. B of Cat. **4.b**, Fig. C of Cat. **4.c** and Fig. D of SEM–EDS analysis of Cat. **4.a**.

The morphology of all the supported catalysts has been studied in SEM instrument equipped with EDS detector. It has been observed in the SEM images of Fe catalyst (Fig. 3A), Ni catalyst (Fig. 3B) and Mn catalyst (Fig. 3C) over HMS, that the particles either have round or hexagonal shape (mean particle size *ca.* $1.20 \pm 0.14\ \mu m$). No substantial difference was observed in the SEM images, even though they are physically different in colour. Therefore, the presence of Fe content was confirmed in the EDS analysis (Fig. 3D). The main peaks are detected as Si at $E_{K\alpha} = 1.72$ keV, Fe at $E_{K\alpha} = 6.43$ and 7.12 keV and Au (sample coating) at $E_{K\alpha} = 2.20$ keV. No crystalline phases of these catalysts are observed in the XRD spectra with Bragg–Bentano geometry (not shown). The low angle XRD power patterns measured for HMS and supported catalysts **4.a**, **4.b** and **4.c** are shown in Fig. 4. All the catalyst and HMS samples exhibited a single low-angle (1 0 0) peak due to the long range order, characteristic of the mesoporous structures. Additionally, the intensity of d_{100} reflection of **4.a**, **4.b** and **4.c** decreased and d_{100} spacing shifted to a higher value, compared with mesoporous HMS. This effect is mainly due to the anchored metal complexes species that occupy the internal pores of HMS by the Fe, Ni and Mn complexes. Therefore, the pore volume of all the supported catalysts should decrease.

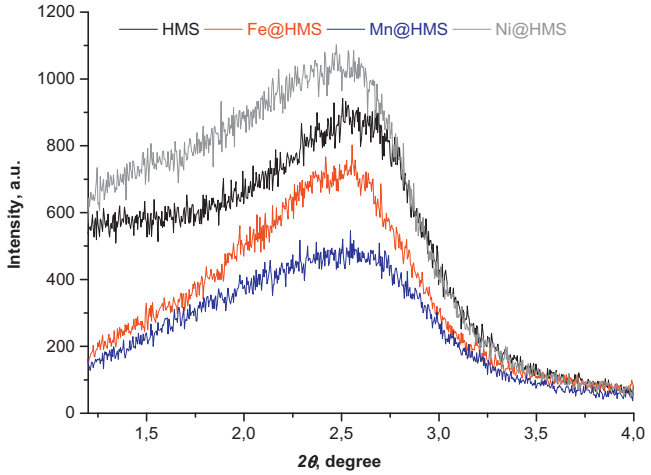

Fig. 4. X-ray diffraction spectra (XRD) of metal complexes into HMS as catalysts (Cat. **4.a**, **4.b** and **4.c**).

3.2. Catalytic oxidation study of cyclohexane

Three types of heterogeneous uniform porous texture HMS supported complex catalysts HMS/Fe[Sal(PMeO-Si)DPTA], **4.a**, HMS/Ni[Sal(PMeO-Si)DPTA], **4.b** and HMS/Mn[Sal(PMeO-Si)DPTA], **4.c** have been applied the in the oxidation reaction of neat cyclohexane by molecular O_2 and obtained ketone in higher amount and alcohol in lower amount. It was also found that they serve as effective heterogeneous catalysts (typical high TONs 4.2×10^3 with **4.a**, 3.4×10^3 with **4.b** and 2.9×10^3 with **4.c**) for such a reaction without the need of using any additive. All the reactions were performed under relatively mild and solvent free conditions in a SS rocking type batch reactor. The Cat.**4.a** provides the best conversion result of the cycloalkane 40.7% with overall KA oil selectivity of 70% in comparison with the other catalysts

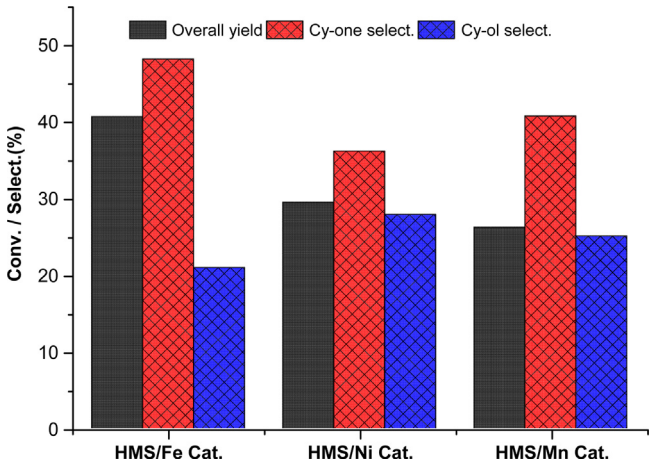

Fig. 5. Effect of metal complexes on percentage conversion and selectivity in the course of cyclohexane oxidation with O_2 (reaction condition = cyclohexane, 27.82 m mol; temp. 423 K; time 4 h, $p(O_2)$ 10 bar; catalyst, 25 mg).

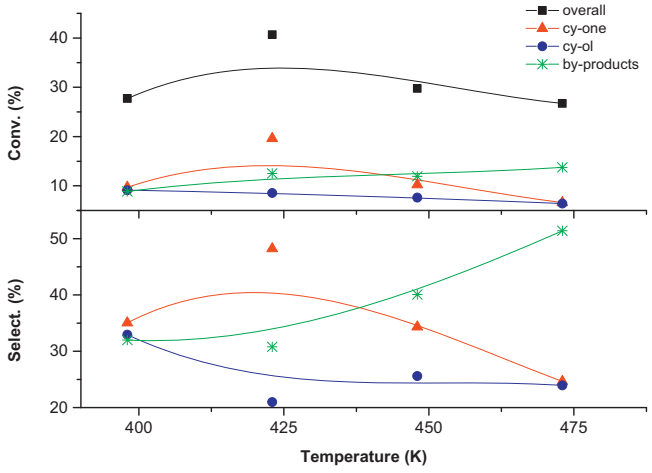

Fig. 6. Temperature effect on the percentage conversion (a) and selectivity (b), of the cyclohexane oxidation products in the presence of the Cat. **4.a** (reaction condition: 10 bar $p(O)_2$, 25 mg catalyst and 27.8 mmol of substrate for 4 h).

(**4.b** and **4.c** compare in Fig. 5, that lead to 29.5 and 26.2% conversion s, respectively). Therefore, we focused our detailed catalytic studies on the Fe based Cat.**4.a**. At the end of oxidation reaction, the colour of Cat.**4.a** was turned from reddish to dark brown, substrate colour from colourless to light yellow and a strong smell of product was also observed. The final reaction mixture was confirmed first in GC and then in GC–MS for identification of products.

Some blank experiments also demonstrate that these catalysts are necessary for the cyclohexane oxidation to process. A low conversion *ca.* 4% was observed when the reaction was carried out without catalyst (analogues condition as Fig. 5). Another experiment with HMS/ligand **2** (without metal) was also performed and we obtained little improved conversion 7.6%. These results suggest that not only metal is responsible for improving the catalytic activity but some other features also play a role in the catalytic oxidation *e.g.* HMS and the structure of complex. The transition state of metal also plays a key role to improve the catalytic efficiency.

On the basis of Fig. 5 results, the detailed catalytic study of cycloalkane process has been carried out with best oxidation Cat. **4.a**. The best reaction condition has been optimized by various temperatures (388–473 K), reaction O_2 pressures (5–20 bar), reaction times (2–14 h) and catalyst amounts (10–55 mg). All the catalytic activity and selectivity results are summarized in Figs. 5–9.

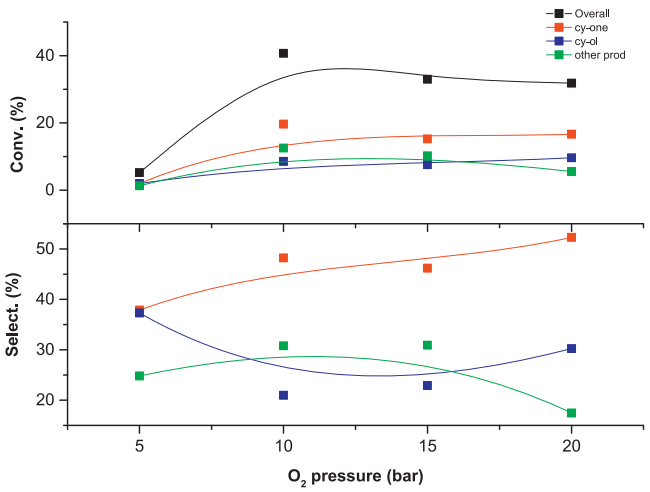

Fig. 7. Pressure effect on the percentage conversion (a) and selectivity (b), of the cyclohexane oxidation products in the presence of the Cat. **4.a** (reaction condition: 423 K temp., 25 mg catalyst and 27.8 mmol of substrate for 4 h).

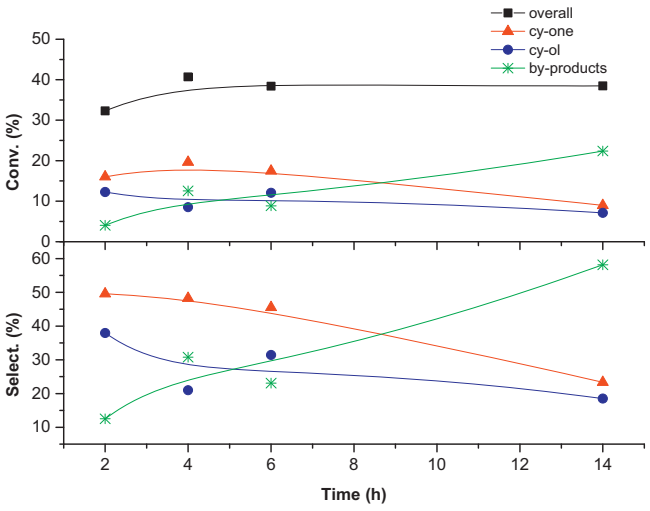

Fig. 8. Time effect on the percentage conversion (a) and selectivity (b), of the cyclohexane oxidation products in the presence of the Cat. **4.a** (reaction condition: 423 temp., 10 bar $p(O)_2$, 25 mg catalyst and 27.8 mmol of substrate).

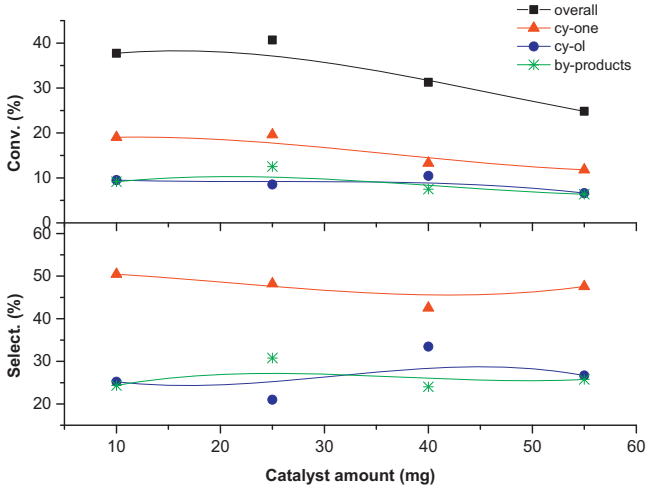

Fig. 9. Amount of catalyst (Cat. **4.a**) effect on the percentage conversion (a) and selectivity (b), of the cyclohexane oxidation products in the presence of the (reaction condition: 423 temp., 10 bar $p(O)_2$ and 27.8 mmol of substrate for 4 h).

Temperature effect on the oxidation of cyclohexane was examined by varying from 398 to 473 K, under constant condition: 27.8 mmol substrate, 4 h time, 10 bar $p(O)_2$ and 25 mg catalyst (Fig. 6). The conversion of product increases slowly at 398 K (overall conversion 27.7%) beyond which it increases sharply until 423 K (overall conversion 40.7%). At higher temperature the overall conversion drops due to the formation of unidentified black material and more by-products (Fig. 6a). Thus in further studies the temperature was not allowed to go above 423 K. At low temperature, 398 K, the cyclo-ol selectivity was higher but after it drops with the increasing of temperature (423–473 K). It is suggesting that the Cy-OOH radicals (intermediate) were initially formed but they were decomposed with the increasing of temperature. At the result, high selectivity of cyclo-one was obtained at 423 K in compare to cyclo-ol. These intermediates (Cy-OOH) were completely decomposed under deep oxidation at 473 K. This was confirmed when the reaction mixture was treated with the excess of PPh_3 before GC analysis [38,39]. The selectivity dependence on the temperature is also shown in pressure effect, $p(O_2)$ on chemical reaction was also investigated in the range from 5 up to 20 bar under constant reaction conditions: 27.8 mmol substrate, 4 h time, 423 K temp., and 25 mg catalyst (Fig. 7). The increase of pressure $p(O_2)$ from 5 up to 10 bar results in the enhancement of overall conversion from 5.2 to 40.7%. Above 10 bar, it was slowly dropping overall conversion 31.5% until at 20 bar for current catalytic system (Fig. 7a). The increasing of main products (cyclo-one and cyclo-ol) selectivities were achieved with the pressure increase of molecular oxygen (above 10 bar). The by-product selectivity was unchanged until 15 bar, then dropped. Therefore, the use of more O_2 pressure is helpful in terms of main products selectivity (Fig. 7b).

Reaction time effect, on the cyclohexane reaction was systematically investigated from 2 up to 14 h with most active Cat. **4.a** under constant reaction conditions: 27.8 mmol substrate, 10 bar $p(O)_2$, 423 K, and 25 mg catalyst (Fig. 8). Initially 32.3% conversion was obtained after 2 h time period, afterwards it increases rapidly and conversion reaches *ca.* 40.7% at 4 h reaction time. After long reaction time (14 h), lower conversion 38.5% (cyclo-one 9.0% plus cyclo-ol 7.1% Fig. 8b) was observed. In the case of selectivity (Fig. 8b), the best result (69.3%) was achieved after 4 h reaction period *i.e.* ketone, 48.2% and alcohol, 21.1%. The extension up to 14 h shows a negative effect on particularly main products selectivity, with concomitantly increment of the by-products.

Catalyst **4.a** amount effect on oxidation reaction was also investigated between 10 up to 55 mg to achieve reaction ideal conditions (constant conditions: 27.8 mmol substrate, 10 bar $p(O)_2$, 423 K and 4 h reaction time, Fig. 9). It was observed that increasing Cat. **4.a** amount from 10 up to 25 mg, the overall conversion increases from 37.7 up to 40.7%. Beyond this amount (25 mg) the overall conversion decreases to 24.8% with 55 mg of catalyst (Fig. 6a). However, the selectivity of main product, *i.e.* cyclo-one, remains always high in compare to other products (Fig. 6a). The selectivity of other desired product (cyclo-ol) and by-products has little change with the increasing amount of catalyst. Therefore, the ratio between catalyst and substrate is an also important factor to maintain a high conversion of desire product.

3.3. Catalyst recycles study

In our catalytic systems, oxygen is a limiting reagent and the catalyst is still active at the end of the reaction and could be recycled or reused even without reactivation. In fact, after performing the oxyfunctization of cyclohexane under the analogous condition as Fig. 6, the reactor was degassed, charged with more O_2 until 10 atm pressure. The reaction was allowed to proceed for a further 4 h period. The overall conversion of alkane then increased *ca.* 12%, relatively to the first runs (40.7%), showing that the system still has considerable catalytic activity after the consumption of O_2. It can be reused for further oxidation batches by admission of more O_2, even without isolating and reactivating the catalyst. However, after being used, the catalyst could be reactivated by heating and recycled, still displaying good catalytic activity. Thus, following cyclohexane oxidation (analogous condition as Fig. 6) for 4 h, the catalyst was separated, reactivated and recycled leading, under the same reaction condition, to an overall 11% conversion reduced. The preservation of some catalytic activity is consistent with the AAS analysis of the supported catalyst that shows only a partial metal leaching upon use. In fact, the freshly supported catalyst **4.a** has 0.16 wt% Fe (see Section 3.1), whereas, after 4 h reaction (analogous condition as Fig. 6), the amount of Fe has reduced to 0.14 wt%.

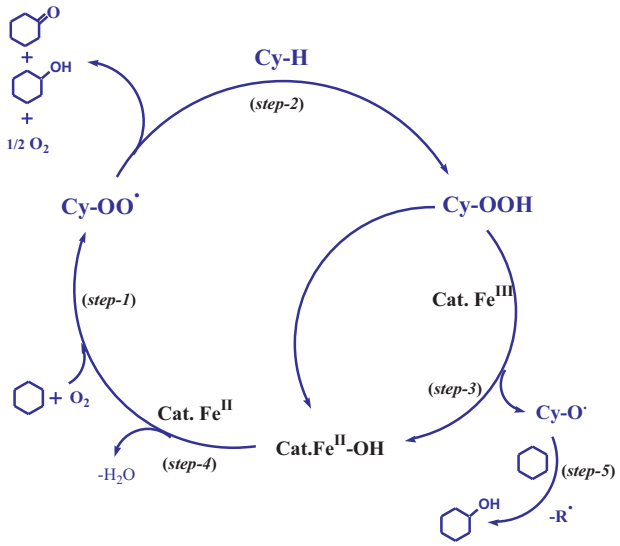

Where, $C_6H_{13}^{\bullet}$ = $Cy^{\bullet}$ = cyclohexyl radical, **Cy-OO•** = cyclohexyl peroxy radical

Scheme 2. Proposed reaction mechanism for cyclo-alkane oxidation.

3.4. Proposed mechanism

The catalytic reaction mechanism is principally depending upon the reaction condition *i.e.* temperature, pressure, liquid or gas phase, the nature of the metal state and the oxidizing agent used [38,40,41]. Therefore, the oxidation mechanism can be divided into three main types: oxidation through coordination of the substrate, catalytic oxygen transfer and oxidation *via* a free radical chain process [40,41]. Although the detailed mechanisms of the reactions are not clear, we believe the current catalytic proceed through free radicals, when the final reaction solution treated with excess PPh_3 in the GC analysis [39]. The Cy-OOH intermediates (in the reaction solution) were deoxygenated by PPh_3 to Cy-OH (formed Ph_3PO), thus suppressing Cy-OOH by the decomposition to both ketone and alcohol in the chromatograph (see Section 2.3) [3,41]. It was further confirm by some additional experiments with radical traps *i.e.* liquid carbon-radical trap ($CBrCl_3$) and oxygen-radical trap (Ph_2NH), analogues condition as Fig. 6. The main product conversion *ca.* 11.3% was dropped, confirms the presence of alkylperoxide intermediates.

Hence the proposed Scheme 2, the cyclohexyl radicals (Cy•) and cyclohexylperoxy radicals (Cy-OO•) can be primarily created by the reaction of molecular O_2 (slowly induction period). Homolytic cleavage of C—H bond of cyclohexane (CyH) can occur by H-abstraction by Cy-OO• to generate a further Cy• and the hydroperoxide Cy-OOH (Step 1), whose homolytic decomposition to Cy-O• and further Cy-OO• (Steps 2 and 3) can be catalyzed by the Fe catalyst. Cy-ol can then be formed by H-atom abstraction

from CyH by the Cy-OO• (Step 4). The Cy-ol can be also formed by the decomposition of Cy-OO• radicals (Step 5). Similar type of mechanism is known to occur for metal catalysts with two oxidation states of comparable stability such as $Mn^{II/III}$, $V^{IV}/^{V}$, $Co^{II/III}$ and $Cu^{I/II}$ [35,40a,b,41]. It is also observe for current catalytic system (catalyst **4.a**) having $Fe^{II/III}$ oxidation states.

4. Conclusions

Three potentially active trimethoxysilane pentacoordinate complexes Fe[Sal(PMeO-Si)DPTA] [**3.a**], Ni[Sal(PMeO-Si)DPTA] [**3.b**] and Mn[Sal(PMeO-Si)DPTA] [**3.c**] were synthesized and characterized. These metal complexes were anchored into HMS without any liker agent. All the supported catalysts **4.a**, **4.b** and **4.c** were systematically tested in the cyclohexane O_2 oxidation process under relatively mild condition in a batch process. Typical high TONs 4.2×10^3 with Fe catalyst **4.a**, 3.4×10^3 with Ni catalyst **4.b** and 2.9×10^3 with Mn catalyst **4.c** were obtained by these supported catalysts. The supported Cat. **4.a** showed highest overall conversion 40.7% with good selective of cyclo-one (48%). These results were obtained under optimize condition (423 K, 10 bar $p(O)_2$, 25 mg catalyst, 27.8 mmol of substrate) in a batch reactor. The TGA showed that these catalysts were stable under the applied temperature (473 K) and they can be recycled further more reactions. Experiments with PPh_3 and initiators provide some supporting testimony in favour of a free-radical mechanism.

Acknowledgements

This work is financially supported by the Fundação para a Ciência e Tecnologia (FCT) of Portugal through projects: PTDC/EQU-ERQ/110825/2009, CQVR/PEst-C/QUI/UI0616/2011 and "*Indian-Portuguese cooperation program-2013*". The authors express gratitude to CACTI Centre Vigo, Spain, and UME/UTAD for catalysts characterizations.

References

[1] Y. Ishii, S. Sakaguchi, T. Iwahama, Adv. Synth. Catal. 343 (2001) 393–427.
[2] (a) G.A. Olah, A. Molnár, Hydrocarbon Chemistry, 3rd ed., Wiley, New York, 2003, pp. 10;
(b) C. Gabriele, C. Fabrizio, T. Ferrucio, Selective Oxidation by Heterogeneous Catalysis, Springer Science + Bussniss Media, New York, 2001.
[3] M.H. Valkenberg, W.F. Hölderich, Catal. Rev. 44 (2002) 321–374.
[4] (a) R. Burch, D.J. Crittle, M.J. Hayes, Catal. Today 47 (1999) 229–234;
(b) R. Burch, M.J. Hayes, J. Mol. Catal. A: Chem. 100 (1995) 13–33.
[5] K.T. Queeney, D.A. Chen, C.M. Friend, Am. Chem. Soc. J. 119 (1997) 6945–6946.
[6] T.F.S. Silva, G.S. Mishra, M.F.G. da Silva, R. Wanke, L.M.D.R.S. Martins, A.J.L. Pombeiro, Dalton Trans. 42 (2009) 9207–9215.
[7] K.M. Parida, M. Sahoo, S. Singha, J. Mol. Catal. A: Chem. 329 (2010) 7–12.
[8] R. Kumar, S. Sithambaram, S.L. Suib, J. Catal. 262 (2009) 304–313.
[9] D. Yang, M. Liu, W. Zhao, L. Gao, Catal. Commun. 9 (2008) 2407–2410.
[10] (a) P.G. Cozzi, Chem. Soc. Rev. 33 (2004) 410–421;
(b) G.C. Salomão, M.H.N. Olsen, V. Drago, C. Fernandes, L.C. Filho, O.A.C. Antunes, Catal. Commun. 8 (2007) 69–72.
[11] T.F.S. Silva, M.F.G. da Silva, G.S. Mishra, L.M.D.R.S. Martins, A.J.L. Pombeiro, J. Organomet. Chem. 696 (2011) 1310–1318.
[12] L. Canali, D.C. Sherrington, Chem. Soc. Rev. 28 (1999) 85–93.
[13] A.R. Silva, M. Martins, M.M.A. Freitas, J.L. Figueiredo, C. Freire, B. de Castro, Eur. J. Inorg. Chem. 10 (2004) 2027–2035.
[14] S.S. Lin, H.S. Weng, Appl. Catal. A: Gen. 118 (1994) 21.
[15] (a) P. Sutra, D. Brunel, Chem. Commun. 21 (1996) 2485–2486;
(b) S. Jana, B. Dutta, R. Bera, S. Koner, Langmuir 23 (2007) 2492–2496;
(c) C.J. Liu, S.G. Li, W.Q. Pang, C.M. Che, Chem. Commun. 1 (1997) 65–66.
[16] C. Gilmartin, J.R.L. Smith, J. Chem. Soc., Perkin Trans. 2 (1995) 243–251.
[17] (a) J. Sandee, L.A. van der Veen, J.N.H. Reek, P.C.J. Kamer, M. Lutz, A.L. Spek, P.W.N.M. van Leeuwen, Angew. Chem. 38 (1999) 3231–3235;
(b) S.R. Hall, C.E. Fowler, B. Lebeau, S. Mann, Chem. Commun. (1999) 201–202.
[18] J.R. Sheehan, Ullmann Encycropedia Industrial Organic Chemicals, vol. 8, Wiley-VCH, Weinhelm, 1999, pp. 4575–4591.
[19] (a) D.E. Mears, A.D. Eastman, in: A. Seidel (Ed.), Kirk-Othmer Encyclopedia of Chemical Technology, vol. 13, 5th ed., John Wiley and Sons, New York, 2004, pp. 706–710;
(b) A.K. Suresh, M.M. Sharma, T. Sridhar, Ind. Eng. Chem. Res. 39 (2000) 3958–3997;
(c) G. Lü, R. Zhao, G. Qian, Y. Qi, X. Wang, J. Suo, Catal. Lett. 97 (2004) 115–118.
[20] R. Whyman, Applied Organometallic Chemistry and Catalysis, Oxford University Press, Oxford, 2001.
[21] A.M. Kirillov, M.N. Kopylovich, M.V. Kirillova, E.Yu. Karabach, M. Haukka, M.F.C.G. da Silva, A.J.L. Pombeiro, Adv. Synth. Catal. 348 (2006) 159–174.
[22] J.M. Bregeault, Dalton Trans. 17 (2003) 3289–3302.
[23] T.M. Salama, I.O. Ali, H.A. Gumaa, Microporous Mesoporous Mater. 113 (2008) 90–98.
[24] S.S. Lin, H.S. Weng, Appl. Catal. A: Gen. 118 (1994) 21–31.
[25] E.L. Pires, J.C. Magalhaes, U. Schuchardt, Appl. Catal. A: Gen. 203 (2000) 231–237.
[26] H. Einaga, S. Futamura, Appl. Catal. B: Environ. 60 (2005) 49.
[27] G.S. Mishra, E.C.B. Alegria, L.R. Martins, A.J.L. Pombeiro, Appl. Catal. A: Gen. 285 (2008) 92–100.
[28] A.A. Susu, F.E. Enoh, A.D.F. Ogunye, J. Chem. Technol. Biotechnol. 30 (1980) 735–747.
[29] G.S. Mishra, S. Sinha, Catal. Lett. 125 (2008) 139–144.
[30] M.R. Maurya, A.K. Chandrakar, S. Chand, J. Mol. Catal. A: Chem. 270 (2007) 225–235.
[31] G.C. Salomaõ, M.H.N. Olsen, V. Drago, C. Fernandes, L.C. Filho, O.A.C. Antunes, Catal. Commun. 8 (2007) 69–72.
[32] G.S. Mishra, A. Kumar, S. Mukhopadhyay, P.B. Tavares, Appl. Catal. A: Gen. 384 (2010) 136–146.
[33] G.S. Mishra, A.J.L. Pombeiro, J. Mol. Catal. A: Chem. 239 (2005) 96–102.
[34] G.S. Mishra, M.J. Lakshmi, A. Kumar, J. Mol. Catal. A: Chem. 230 (1–2) (2005) 35–42.
[35] A. KumarJr, G.S. Mishra, A. Kumar, Trans. Met. Chem. 28 (8) (2003) 913–917.
[36] F. Carré, R.J.P. Corriu, E.L. Beltran, A. Mehdi, C. Reyé, R. Guilard, J. Sýkora, A. van der Lee, Dalton Trans. 16 (2003) 3211–3215.
[37] (a) P.T. Tanev, T.J. Pinnavaia, Science 267 (1995) 865;
(b) B. Jarrais, C. Pereira, A.R. Silva, A.P. Carvalho, J. Pires, C. Freire, Polyhedron 28 (2009) 994–1000.
[38] M. Nowothny, L.N. Pedersen, U. Hanefeld, T. Maschmeyer, Chem. Eur. J. 8 (2002) 3724–3730.
[39] M. Vennat, P. Herson, J.M. Bregeault, G.B. Shul'pin, Eur. J. Inorg. Chem. 5 (2003) 908–917.
[40] (a) C.A. Tolman, J.D. Druliner, M.J. Nappa, N. Herron, in: C.L. Hill (Ed.), Activation Functionalization of Alkanes, Wiley, New York, 1989, pp. 303–360;
(b) M. Hartman, S. Ernst (Eds.), Angew. Chem. Int. 39 (2000) 888–890;
(c) M. Spielman, AIChE J. 10 (1964) 496–501;
(d) C.A. Tolman, J.D. Druliner, P.J. Krisic, M.J. Nappa, W.C. Seidel, I.D. Williams, S.D. Ittel, J. Mol. Catal. 48 (1988) 129–148;
(e) A. Kumar, G.S. Mishra, A. Kumar, Trans. Met. Chem. 28 (2003) 913–917;
(f) R. Pohorecki, J. Ba, W. Dyga, W. Moniuk, A. Podgorska, P. Zdrojkowski, Wierzchowski, Chem. Eng. Sci. 56 (2001) 1285–1391.
[41] (a) U. Schuchardt, D. Cardoso, R. Sercheli, R. Pereira, R.S. Da Cruz, M.C. Mario, D. Mandelli, E.V. Spinace, E.L. Pires, Appl. Catal. A: Gen. 211 (2001) 1–17;
(b) K. Machado, A. Kumar, G.S. Mishra, J. Ind. Eng. Chem. (2013), http://dx.doi.org/10.1016/j.jiec.2013.09.055 (in press);
(c) G.S. Nunes, I. Mayer, H.E. Toma, K. Araki, J. Catal. 236 (2005) 55–61;
(d) E.I. Karasevish, Yu.K. Karasevish, Kinet. Catal. 41 (2000) 535–542;
(e) A. Maldotti, C. Bartocci, G. Varani, A. Molinari, P. Battioni, D. Mansuy, Inorg. Chem. 35 (1996) 1126–1131.